Translational and rotational relative dynamics modeling and its use in spacecraft rendezvous with an uncertain docking port location

Miguel Castroviejo-Fernandez*, Michele Ambrosino†, and Ilya Kolmanovsky‡
University of Michigan, Ann Arbor, MI 48109-2140, USA

Himadri Basu§, and Ricardo G. Sanfelice¶
University of California Santa Cruz, Santa Cruz, CA 95060, USA

This paper considers control-oriented modeling of the relative motion and orientation of a deputy spacecraft with respect to a chief spacecraft in circular orbit. We present equations in the form which relates the relative position of a point of interest on the deputy spacecraft with respect to the center of mass of the chief spacecraft. The deputy spacecraft is assumed to be equipped with thrusters and reaction wheels. Conditions under which a discrete-time periodic linear system model can be obtained from the nonlinear one are given. A simulation case study is presented which illustrates the usefulness of the considered model in performing rendezvous maneuvers to an unknown docking port on a rotating chief spacecraft.

I. Introduction

The interest in spacecraft relative motion and rendezvous maneuvers is growing concomitantly with the growing number of space missions. These can serve the purposes of exploration, on-orbit refueling and servicing as well as satellite decommissioning. Moreover, due to the remoteness of the space environment, autonomous rendezvous maneuvers are, in particular, attractive. In the context of spacecraft rendezvous, it is common to consider a deputy spacecraft docking to a chief spacecraft. In general, the chief spacecraft may be non-cooperative, can exhibit rotation and, moreover, the location of a potential docking port on the chief spacecraft may be unknown. In this case, it is important for the controlled space vehicle, i.e. the deputy, to simultaneously identify the docking port location prior to or while executing the rendezvous maneuver.

Docking port estimation is in itself a challenging problem involving not only control but also on-board perception aspects. Recently, the digital twin (DT) formalism [1–3], and, in particular, the predictive DT formalism [4], have been proposed as a way to centralize the different digital agents needed for accurate control and monitoring of physical systems. The DT exploits sensor measurement data and keeps an updated digital model as well as estimates of the system state and other quantities of interest. It can also provide reference trajectories to the controller and, in general, the controller can also be considered as a part of the DT framework. Depending on the model used in the DT, the target reference trajectory can be more complex or even highly time-varying. Therefore, it is crucial to appropriately choose the dynamical model of the physical system to simplify the implementation.

In this work, we consider a rendezvous maneuver to a chief spacecraft in a circular orbit and rotating at a constant rate in the Hill's relative motion frame [5]. In the same setting, reference [6] derived coupled translational and rotational dynamics for the relative position of a point of interest on the deputy spacecraft with respect to a point of interest on the chief spacecraft. Reference [7] developed coupled dynamics for the more general case of elliptic orbits but assuming that the chief spacecraft was not rotating in the Hill's frame. In [6], it is assumed that the location of the point of interest on the chief spacecraft , i.e., the chief docking port, is known and enters explicitly into the dynamics. However, we assume the point of interest on the chief to be unknown which complicates the use of the equations of motion (EoMs) derived in [6]. To account for this, we derive a similar set of equations that represents the dynamics of the relative position to the center of mass of the chief spacecraft. We then derive the equilibrium manifold for the resulting system

*PhD Student, Department of Aerospace Engineering
†Postdoctoral Fellow, Department of Aerospace Engineering
‡Professor, Department of Aerospace Engineering, AIAA Associate Fellow
§Postdoctoral Fellow, Department of Electrical and Computer Engineering
¶Professor, Department of Electrical and Computer Engineering

and show that the point of interest can be reached by selecting an appropriate constant reference command. This is beneficial for the problem considered here as the unknown docking port does not enter the dynamics directly and instead can be seen as an uncertain reference command. Moreover, we consider the addition of a reaction wheel (RW) array for the EoM derivation. We illustrate the advantages of using the derived dynamics for the pre-capture phase in a rendezvous maneuver to a rotating chief spacecraft with initially unknown docking port. This is done through the design of a feedback controller and the generation of an appropriate reference trajectory that first locates the approximate docking port position and then ensures proper advancement to it. The reference trajectory generation and docking port position estimation are assumed to be handled by a DT or other external module.

In Section II, the coupled translational and rotational dynamics are derived. Section III describes the equilibria manifold and a linearization and discretization approach for the system considered. Then, Section IV show casts, through a case study, the usefulness of the proposed equations.

Notations: Let $\vec{\cdot}$ denote a physical vector. Given a frame $\mathcal{F}$, and a physical vector $\vec{c}$ then $\vec{c}|_{\mathcal{F}}$ is the resolution of $\vec{c}$ in frame $\mathcal{F}$. Moreover, $\overset{\mathcal{F}\cdot}{\vec{c}}$ is the time derivative of $\vec{c}$ with respect to frame $\mathcal{F}$, similarly for $\overset{\mathcal{F}\cdot\cdot}{\vec{c}}$. Given $c = \vec{c}|_{\mathcal{F}}$ then $\dot{c} = \overset{\mathcal{F}\cdot}{\vec{c}}|_{\mathcal{F}}$. A physical matrix $\vec{M}$ is such that $\vec{M} = \sum_{i=1}^{n} \vec{x}_i \vec{x}_{i+n}^{\top}$, where $\{\vec{x}_i\}_{i=1}^{2n}$ are $2n$ physical vectors, then $\vec{M}|_{\mathcal{F}} = \sum_{i=1}^{n} \vec{x}_i|_{\mathcal{F}} \vec{x}_{i+n}|_{\mathcal{F}}^{\top}$. Moreover, the rank of $\vec{M}$ is equal to the rank of $\vec{M}|_{\mathcal{F}}$ for any orthonormal frame $\mathcal{F}$. Moreover if $\vec{M}$ is full rank, $\vec{M}^{-1}$ is such that $\vec{M}^{-1}|_{\mathcal{F}} = \vec{M}|_{\mathcal{F}}^{-1}$. For any $a \in \mathbb{R}^n$, $b \in \mathbb{R}^m$ then $(a, b) = [a^{\top}, b^{\top}]^{\top}$. For any $v \in \mathbb{R}^3$ such that $v = (v_1, v_2, v_3)$,

$$v^{\times} = \begin{bmatrix} 0 & -v_3 & v_2 \\ v_3 & 0 & -v_1 \\ -v_2 & v_1 & 0 \end{bmatrix}.$$

II. Relative dynamics

A. Setting

Consider a chief spacecraft and deputy spacecraft orbiting around the Earth. We assume that both spacecrafts are rigid and that the Earth's gravity is the only external force nominally acting on the vehicles. Thus, the motion of each spacecraft CoM can be described using the two body problem equations of motion. Moreover, the chief is assumed to be uncontrolled and its CoM follows a circular orbit with mean motion parameter, n. On the contrary, the deputy spacecraft is equipped with three orthogonally oriented thrusters and with three RWs located at its CoM with axis of rotation aligned with the principal moments of inertia.

In this section we aim to derive a set of equations describing the relative position of a point of interest (i.e., docking port) on the deputy spacecraft with respect to the CoM of the chief spacecraft. As stated in the introduction, the EoMs are based on [6] and, for the sake of completeness, we summarize the derivations here. The relationship between the EoMs derived in [6] and the ones here is described in Remark 1. We first introduce the following frames that will be used in the derivation of the EoMs.

B. Reference frames

An illustration of the different orthogonal frames is found on Figure 1. More specifically:

- $\mathcal{I}$: inertial frame with the origin at center of the Earth.
- $\mathcal{T}$: rotating frame with the origin at CoM of chief spacecraft and rotating at angular rate n, i.e., a Local Vertical Local Horizontal frame (LVLH).
- $\mathcal{C}$: rotating frame fixed to the bus of the chief spacecraft.
- $\mathcal{D}$: rotating frame fixed to the bus of the deputy spacecraft.
- $\mathcal{W}_i,\ i = 1, 2, 3$: rotating frame fixed to the i^{th} reaction wheel.

Frames $\mathcal{C},\ \mathcal{D}$ have axes aligned with principal axes of the chief and deputy spacecrafts, respectively. Frames $\mathcal{W}_i$ have each an axis aligned with the axis of rotation of the corresponding RW in frame $\mathcal{D}$.

C. Translational dynamics

The two body problem EoMs for the chief and deputy spacecrafts are given by

$$
{}^{\mathcal{I}}\ddot{\vec{r}}_c = \frac{-\mu}{R_c^3}\vec{r}_c, \tag{1a}
$$

$$
{}^{\mathcal{I}}\ddot{\vec{r}}_d = \frac{-\mu}{R_d^3}\vec{r}_d + \frac{\vec{F}_d}{m_d}, \tag{1b}
$$

where $\vec{r}_c,\ \vec{r}_d$ are the physical vectors from the earth CoM to the CoM of the chief and deputy spacecraft, respectively, and $R_c = \|\vec{r}_c\|,\ R_d = \|\vec{r}_d\|$, μ is the gravitational parameter of the Earth and $\vec{F}_d$ are the control forces acting on the deputy spacecraft.

Define $\vec{\rho}_0 = \vec{r}_d - \vec{r}_c$, i.e., $\vec{\rho}_0$ is the physical vector for the position of the deputy CoM relative to the chief CoM. From (1), we directly obtain

$$
{}^{\mathcal{I}}\ddot{\vec{\rho}}_0 = \frac{\mu}{R_c^3}\vec{r}_c - \frac{\mu}{R_d^3}\vec{r}_d + \frac{\vec{F}_d}{m_d} = \frac{\mu(R_d^3 - R_c^3)}{R_d^3 R_c^3}\vec{r}_c - \frac{\mu}{R_d^3}\vec{\rho}_0 + \frac{\vec{F}_d}{m_d}. \tag{2}
$$

Moreover, using the transport theorem we have that

$$
{}^{\mathcal{I}}\ddot{\vec{\rho}}_0 = {}^{\mathcal{T}}\ddot{\vec{\rho}}_0 + {}^{\mathcal{T}}\dot{\vec{\omega}}_{\mathcal{T}/\mathcal{I}} \times \vec{\rho}_0 + 2\vec{\omega}_{\mathcal{T}/\mathcal{I}} \times {}^{\mathcal{T}}\dot{\vec{\rho}}_0 + \vec{\omega}_{\mathcal{T}/\mathcal{I}} \times (\vec{\omega}_{\mathcal{T}/\mathcal{I}} \times \vec{\rho}_0), \tag{3}
$$

where $\vec{\omega}_{\mathcal{T}/\mathcal{I}}$ is the angular velocity of frame $\mathcal{T}$ with respect to frame $\mathcal{I}$. Replacing (3) in (2) we get

$$
{}^{\mathcal{T}}\ddot{\vec{\rho}}_0 = \frac{\mu(R_d^3 - R_c^3)}{R_d^3 R_c^3}\vec{r}_c - \frac{\mu}{R_d^3}\vec{\rho}_0 + \frac{\vec{F}_d}{m_d} - {}^{\mathcal{T}}\dot{\vec{\omega}}_{\mathcal{T}/\mathcal{I}} \times \vec{\rho}_0 - 2\vec{\omega}_{\mathcal{T}/\mathcal{I}} \times {}^{\mathcal{T}}\dot{\vec{\rho}}_0 - \vec{\omega}_{\mathcal{T}/\mathcal{I}} \times (\vec{\omega}_{\mathcal{T}/\mathcal{I}} \times \vec{\rho}_0). \tag{4}
$$

Let us introduce the variables

$$
\omega_t = \vec{\omega}_{\mathcal{T}/\mathcal{I}}|_{\mathcal{T}}, \dot{\omega}_t = {}^{\mathcal{T}}\dot{\vec{\omega}}_{\mathcal{T}/\mathcal{I}}|_{\mathcal{T}},\ F_d = \vec{F}_d|_{\mathcal{D}},\ \rho_0 = \vec{\rho}_0|_{\mathcal{T}},\ r_c = \vec{r}_c|_{\mathcal{T}},\ Q = O_{\mathcal{D}/\mathcal{C}},\ R = O_{\mathcal{C}/\mathcal{T}}. \tag{5}
$$

Resolving (4) in frame $\mathcal{T}$, we get:

$$
{}^{\mathcal{T}}\ddot{\vec{\rho}}_0|_{\mathcal{T}} = \ddot{\rho}_0 = \frac{\mu(R_d^3 - R_c^3)}{R_d^3 R_c^3} r_c - \frac{\mu}{R_d^3}\rho_0 + \frac{R^\top Q^\top F_d}{m_d} - \dot{\omega}_t \times \rho_0 - 2\omega_t \times \dot{\rho}_0 - \omega_t \times (\omega_t \times \rho_0). \tag{6}
$$

Given the chief is in a circular orbit with parameter $n^2 = \frac{\mu}{R_c^3}$ we have that $\omega_t = [0\ 0\ -n]^\top$ and $\dot{\omega}_t = 0$. Moreover, assuming that the norm of the relative position of the CoMs is much smaller than R_c, the linearization of (6) gives the Clohessy–Wiltshire-Hill (CWH) equations [5]:

$$
\ddot{\rho}_0 = G_1\rho_0 + G_2\dot{\rho}_0 + \frac{R^\top Q^\top F_d}{m_d}, \tag{7}
$$

where $G_1 = \begin{bmatrix} 3n^2 & 0 & 0 \\ 0 & 0 & 0 \\ 0 & 0 & -n^2 \end{bmatrix}, G_2 = \begin{bmatrix} 0 & -2n & 0 \\ 2n & 0 & 0 \\ 0 & 0 & 0 \end{bmatrix}$. In this work we are interested in the relative position of an arbitrary point on the deputy spacecraft relative to the CoM of the chief spacecraft (see Figure 2). We define

$$
\vec{\rho} = \vec{P}_d + \vec{\rho}_0, \tag{8}
$$

where $\vec{P}_d$ is the relative position of the arbitrary point of interest with respect to the CoM of deputy. We define $\vec{\rho}|_{\mathcal{C}} = \rho,\ \vec{P}_d|_{\mathcal{D}} = P_d$ and $\vec{\omega}_{\mathcal{C}/\mathcal{T}}|_{\mathcal{C}} = \omega_c,\ {}^{\mathcal{C}}\dot{\vec{\omega}}_{\mathcal{C}/\mathcal{T}}|_{\mathcal{C}} = \dot{\omega}_c, \vec{\omega}_{\mathcal{D}/\mathcal{C}}|_{\mathcal{D}} = \omega,\ {}^{\mathcal{C}}\dot{\vec{\omega}}_{\mathcal{D}/\mathcal{C}}|_{\mathcal{D}} = \dot{\omega}$. We then have that

$$
\rho_0 = R^\top(\rho) - R^\top Q^\top P_d, \tag{9a}
$$

$$
\dot{\rho}_0 = {}^{\mathcal{T}}\dot{\vec{\rho}}|_{\mathcal{T}} - {}^{\mathcal{T}}\dot{\vec{P}}_d|_{\mathcal{T}} = R^\top(\dot{\rho} + \omega_c \times \rho) - R^\top Q^\top(\omega + Q\omega_c) \times P_d, \tag{9b}
$$

and, additionally:

$$\begin{aligned}\ddot{\rho}_0 =& R^\top(\ddot{\rho} + 2\omega_c \times \dot{\rho} + \dot{\omega}_c \times \rho + \omega_c \times (\omega_c \times \rho)) \\ & - R^\top Q^\top((\dot{\omega} + Q(\dot{\omega}_c) - (Q^\top\omega)\times\omega_c)\times P_d + \omega_c \times ((\omega + Q\omega_c)\times P_d)).\end{aligned} \tag{9c}$$

Combining (9) and (7), we obtain the coupled translational relative motion equation resolved in frame C:

$$\begin{aligned}\ddot{\rho} =& RG_1R^\top(\rho - Q^\top P_d) + RG_2R^\top\dot{\rho} + \frac{Q^\top}{m_d}F_d + RG_2R^\top\left[\omega_c \times \rho - Q^\top\big((\omega + Q\omega_c)\times P_d\big)\right] \\ & - 2\omega_c \times \dot{\rho} - \dot{\omega}_c \times \rho - \omega_c \times (\omega_c \times (\rho + P_c)) \\ & + Q^\top\left[\big(\dot{\omega} + Q(\dot{\omega}_c - (Q^\top\omega)\times\omega_c)\big)\times P_d + (\omega + Q\omega_c)\times((\omega + Q\omega_c)\times P_d)\right].\end{aligned}$$

D. Rotational kinematics

The orientation of $\mathcal{D}$ with respect to C is characterized using quaternions with structure $q = [\bar{q}^\top \; q_4]^\top$. The direction cosine matrix corresponding to this rotation is given by

$$\mathcal{R}(\bar{q}, q_4) = \begin{bmatrix} q_1^2 - q_2^2 - q_3^2 + q_4^2 & 2(q_1q_2 + q_3q_4) & 2(q_1q_3 - q_2q_4) \\ 2(q_1q_2 - q_3q_4) & -q_1^2 + q_2^2 - q_3^2 + q_4^2 & 2(q_2q_3 + q_1q_4) \\ 2(q_1q_3 + q_2q_4) & 2(q_2q_3 - q_1q_4) & -q_1^2 - q_2^2 + q_3^2 + q_4^2 \end{bmatrix}, \tag{10}$$

and, additionally, we have the following kinematic equations for the quaternions:

$$\dot{\bar{q}} = \frac{1}{2}(\bar{q}^\times + q_4 I_3)\omega, \tag{11a}$$

$$\dot{q}_4 = -\frac{1}{2}\bar{q}^\top\omega. \tag{11b}$$

The orientation of frame C with respect to $\mathcal{T}$ and ω_c can be characterized in a similar way.

E. Rotational dynamics

We have,

$$\overset{\mathcal{I}\cdot}{\vec{\omega}}_{\mathcal{D}/\mathcal{I}} - \overset{\mathcal{I}\cdot}{\vec{\omega}}_{C/\mathcal{I}} = \overset{\mathcal{I}\cdot}{\vec{\omega}}_{\mathcal{D}/C} = \overset{\mathcal{D}\cdot}{\vec{\omega}}_{\mathcal{D}/C} + \vec{\omega}_{\mathcal{D}/\mathcal{I}} \times \vec{\omega}_{\mathcal{D}/C}.$$

Noting that $\overset{\mathcal{I}\cdot}{\vec{\omega}}_{\mathcal{D}/\mathcal{I}} = \overset{\mathcal{D}\cdot}{\vec{\omega}}_{\mathcal{D}/\mathcal{I}}$, $\overset{\mathcal{I}\cdot}{\vec{\omega}}_{C/\mathcal{I}} = \overset{C\cdot}{\vec{\omega}}_{C/\mathcal{I}}$ we then get

$$\overset{\mathcal{D}\cdot}{\vec{\omega}}_{\mathcal{D}/C} = \overset{\mathcal{D}\cdot}{\vec{\omega}}_{\mathcal{D}/\mathcal{I}} - \overset{C\cdot}{\vec{\omega}}_{C/\mathcal{I}} - \vec{\omega}_{\mathcal{D}/\mathcal{I}} \times \vec{\omega}_{\mathcal{D}/C}. \tag{12}$$

The Euler equations for the chief spacecraft are given by

$$\vec{J}_c \overset{C\cdot}{\omega}_{C/\mathcal{I}} = -\vec{\omega}_{C/\mathcal{I}} \times \vec{J}_c \vec{\omega}_{C/\mathcal{I}}. \tag{13}$$

For the deputy, we assume that the RWs have zero transversal moments of inertia and identical moments of inertia along the axis of rotation. We define $\vec{J}_d = \vec{J}_d^b + \sum_{i=1}^3 J_i^{rw}$, where $\vec{J}_d$ is the physical inertia matrix of the deputy, $\vec{J}_d^b$ is the physical inertia matrix of the deputy spacecraft bus and J_i^{rw} is that of the i^{th} RW. For the spacecraft bus we have,

$$\overset{\mathcal{I}\cdot}{H}{}^b_{\mathcal{I}} = \vec{J}_d^b \overset{\mathcal{D}\cdot}{\vec{\omega}}_{\mathcal{D}/\mathcal{I}} + \vec{\omega}_{\mathcal{D}/\mathcal{I}} \times J_d^b \vec{\omega}_{\mathcal{D}/\mathcal{I}}, \tag{14}$$

and for the i^{th} reaction wheel:

$$H_{\mathcal{I}}^{rw} = \vec{J}_i^{rw}(\vec{\omega}_{\mathcal{W}_i/\mathcal{D}} + \vec{\omega}_{\mathcal{D}/\mathcal{I}}) \tag{15a}$$

$$\overset{\mathcal{I}\cdot}{H}{}^{rw}_{\mathcal{I}} = \vec{J}_i^{rw} \overset{\mathcal{D}\cdot}{\vec{\omega}}_{\mathcal{W}_i/\mathcal{I}} + \vec{\omega}_{\mathcal{D}/\mathcal{I}} \times J_i^{rw}(\vec{\omega}_{\mathcal{W}_i/\mathcal{D}} + \vec{\omega}_{\mathcal{D}/\mathcal{I}}) \tag{15b}$$

$$= \vec{J}_i^{rw} \overset{\mathcal{D}\cdot}{\vec{\omega}}_{\mathcal{D}/\mathcal{I}} + \vec{\omega}_{\mathcal{D}/\mathcal{I}} \times J_i^{rw}\vec{\omega}_{\mathcal{D}/\mathcal{I}} + \vec{J}_i^{rw} \overset{\mathcal{D}\cdot}{\vec{\omega}}_{\mathcal{W}_i/\mathcal{D}} + \vec{\omega}_{\mathcal{D}/\mathcal{I}} \times J_i^{rw}\vec{\omega}_{\mathcal{W}_i/\mathcal{D}}. \tag{15c}$$

The Euler equation of rotation for the deputy spacecraft is then given by

$$\overset{\mathcal{I}\cdot}{H^b}_{\mathcal{I}} + \sum_{i=1}^{3} \overset{\mathcal{I}\cdot}{H}{}^{rw}_{\mathcal{I}} = \vec{M}_d, \tag{16}$$

where $\vec{M}_d$ is the physical vector of external moments acting on the deputy about the CoM. Moments induced by the thrusters can be included in this term. Using (15) we get,

$$\vec{J}_d \overset{\mathcal{D}\cdot}{\vec{\omega}}_{\mathcal{D}/\mathcal{I}} = \vec{M}_d - \vec{\omega}_{\mathcal{D}/\mathcal{I}} \times (\vec{J}_d \vec{\omega}_{\mathcal{D}/\times I}) - \sum_{i=1}^{3} \left(\vec{J}_i^{rw} \overset{\mathcal{D}\cdot}{\vec{\omega}}_{\mathcal{W}_i/\mathcal{D}} + \vec{\omega}_{\mathcal{D}/\mathcal{I}} \times \vec{J}_i^{rw} \vec{\omega}_{\mathcal{W}_i/\mathcal{D}} \right). \tag{17}$$

From (13), (17) and (12) we get,

$$\begin{aligned} \overset{\mathcal{D}\cdot}{\vec{\omega}}_{\mathcal{D}/C} &= \vec{J}_d^{-1} \vec{M}_d - \vec{J}_d^{-1} \vec{\omega}_{\mathcal{D}/\mathcal{I}} \times (\vec{J}_d \vec{\omega}_{\mathcal{D}/\mathcal{I}}) + \vec{J}_c^{-1} \vec{\omega}_{C/\mathcal{I}} \times \vec{J}_c \vec{\omega}_{C/\mathcal{I}} - \vec{\omega}_{\mathcal{D}/\mathcal{I}} \times \vec{\omega}_{\mathcal{D}/C} \\ &\quad - \vec{J}_d^{-1} \sum_{i=1}^{3} \left(\vec{J}_i^{rw} \overset{\mathcal{D}\cdot}{\vec{\omega}}_{\mathcal{W}_i/\mathcal{D}} + \vec{\omega}_{\mathcal{D}/\mathcal{I}} \times \vec{J}_i^{rw} \vec{\omega}_{\mathcal{W}_i/\mathcal{D}} \right). \end{aligned} \tag{18}$$

We define $\vec{J}_c|_C = J_c,\ \vec{J}_d|_{\mathcal{D}} = J_d,\ \vec{J}_i^{rw}|_{\mathcal{D}} = J_i^{rw},\ \vec{M}_d|_{\mathcal{D}} = M_d$ as well as $\vec{\omega}_{\mathcal{W}_i/\mathcal{D}}|_{\mathcal{D}} = \Omega_i,\ \overset{\mathcal{D}\cdot}{\vec{\omega}}_{\mathcal{W}_i/\mathcal{D}}|_{\mathcal{D}} = \dot{\Omega}_i,\ i = 1, 2, 3$. Furthermore we have that $\vec{\omega}_{\mathcal{D}/\mathcal{I}}|_{\mathcal{D}} = \omega + Q\omega_c + QR\omega_t$ and $\vec{\omega}_{C/\mathcal{I}}|_{\mathcal{D}} = Q\omega_c + QR\omega_t$. We then get for (18) resolved in frame $\mathcal{D}$:

$$\begin{aligned} \dot{\omega} &= J_d^{-1} \left[M_d - (\omega + Q\omega_c + QR\omega_t) \times J_d(\omega + Q\omega_c + QR\omega_t) \right] + QJ_c^{-1} \left[(\omega_c + R\omega_t) \times J_c(\omega_c + R\omega_t) \right] \\ &\quad - (Q\omega_c + QR\omega_t) \times \omega - J_d^{-1} \sum_{i=1}^{3} \left(J_i^{rw} \dot{\Omega}_i + (\omega + Q\omega_c + QR\omega_t) \times J_i^{rw} \Omega_i \right). \end{aligned}$$

F. Summary of the dynamics

The translational and rotational EoMs derived above are summarized hereunder:

$$\begin{aligned} \ddot{\rho} &= RG_1 R^\top (\rho - Q^\top P_d) + RG_2 R^\top \dot{\rho} + RG_2 R^\top \left[\omega_c \times \rho - Q^\top \left((\omega + Q\omega_c) \times P_d \right) \right] \\ &\quad + \frac{Q^\top}{m_d} F_d - 2\omega_c \times \dot{\rho} - \dot{\omega}_c \times \rho - \omega_c \times (\omega_c \times (\rho + P_c)) \\ &\quad + Q^\top \left[\left(\dot{\omega} + Q(\dot{\omega}_c - (Q^\top \omega) \times \omega_c) \right) \times P_d + (\omega + Q\omega_c) \times ((\omega + Q\omega_c) \times P_d) \right], \end{aligned} \tag{19a}$$

$$\dot{\bar{q}} = \frac{1}{2} (\bar{q}^\times + q_4 I_3) \omega, \tag{19b}$$

$$\dot{q}_4 = -\frac{1}{2} \bar{q}^\top \omega, \tag{19c}$$

$$Q = \mathcal{R}(\bar{q}, q_4), \tag{19d}$$

$$\dot{\bar{p}} = \frac{1}{2} (\bar{p}^\times + p_4 I_3) \omega_c, \tag{19e}$$

$$\dot{p}_4 = -\frac{1}{2} \bar{p}^\top \omega_c, \tag{19f}$$

$$R = \mathcal{R}(\bar{p}, p_4), \tag{19g}$$

$$\begin{aligned} \dot{\omega} &= J_d^{-1} \left[M_d - (\omega + Q\omega_c + QR\omega_t) \times J_d(\omega + Q\omega_c + QR\omega_t) \right] \\ &\quad + QJ_c^{-1} \left[(\omega_c + R\omega_t) \times J_c(\omega_c + R\omega_t) \right] - (Q\omega_c + QR\omega_t) \times \omega \\ &\quad - J_d^{-1} \sum_{i=1}^{3} \left(J_i^{rw} \dot{\Omega}_i + (\omega + Q\omega_c + QR\omega_t) \times J_i^{rw} \Omega_i \right). \end{aligned} \tag{19h}$$

The relevant reference frames are depicted in Figure 1 and the physical vectors of interest are shown in Figure 2. Moreover, we note that:

- P_d is the position of the point of interest of the deputy spacecraft resolved in frame $\mathcal{D}$;
- ρ is the relative position of point $\vec{P}_d$ with respect to the CoM of the chief spacecraft resolved in frame C;
- $(\bar{q}^\top, q_4)^\top$ is the quaternion parameterizing the rotation between frames $\mathcal{D}$ and C;
- $(\bar{p}^\top, p_4)^\top$ is the quaternion parameterizing the rotation between frames C and $\mathcal{T}$;
- $\mathcal{R}$ maps an appropriate quaternion into the orientation matrix it characterizes see (10);
- R, Q are orientation matrices between C -$\mathcal{T}$ and between $\mathcal{D}$ - C, respectively;
- F_d is the vector of control forces resolved in frame $\mathcal{D}$;
- G_1, G_2 are coefficient matrices given in (7);
- $\omega, \omega_c, \omega_t$ are the angular velocity of $\mathcal{D}$ relative to C; of C relative to $\mathcal{T}$ and of $\mathcal{T}$ relative to $\mathcal{I}$, respectively;
- J_d, J_c are the matrices of moment of inertia of the deputy resolved in frame $\mathcal{D}$ and of the chief resolved in frame C;
- J_i^{rw} are the matrices of moment of inertia of the i^{th} reaction wheel resolved in frame $\mathcal{D}$;
- $\Omega_i, \dot{\Omega}_i$ are the angular velocities and angular accelerations of the i^{th} reaction wheel with respect to frame $\mathcal{D}$;
- M_d is the vector of control moments acting on the deputy spacecraft at the CoM, resolved in frame $\mathcal{D}$.

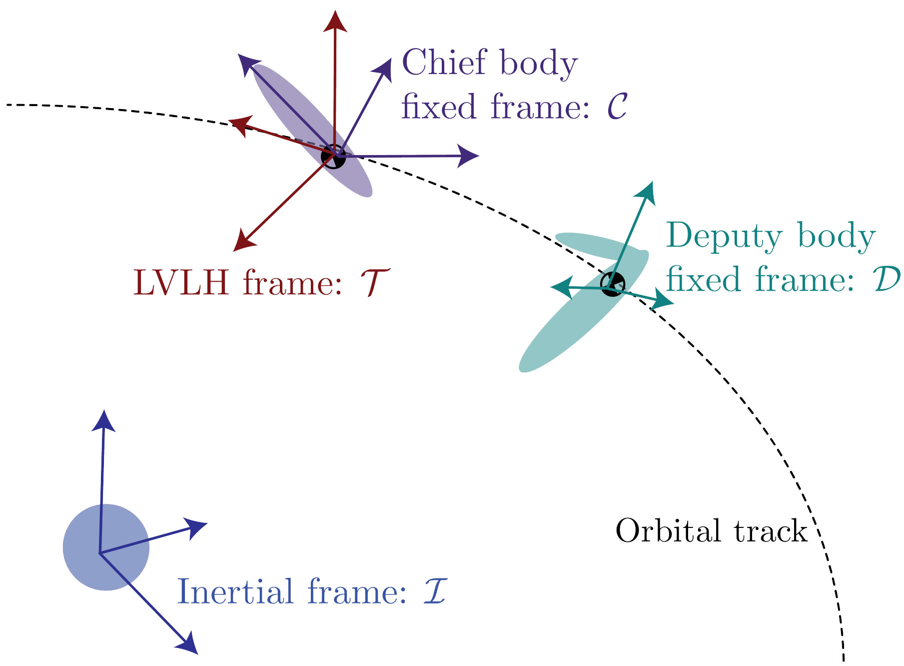

Fig. 1 Different frames used to derive the relative dynamics

Remark 1 *Note that if we are interested in the relative position of $\vec{P}_d$ with respect to $\vec{P}_c$, where $\vec{P}_c$ is an arbitrary point on the chief spacecraft we may define $\vec{\rho}_1 = \vec{\rho}_0 - \vec{P}_c + \vec{P}_d$ or, equivalently, $\vec{\rho}_1 - \vec{P}_c = \vec{\rho}$. Defining $P_c = \vec{P}_c|_C$ and noting that $\overset{C\cdot\cdot}{\rho} = \overset{C\cdot\cdot}{\rho}_1$, we can directly get the dynamics describing the evolution of ρ_1 from* (19a). *This and assuming $\Omega_i = \dot{\Omega}_i = 0$ corresponds to the EoMs derived in [6]. Conversely, in the case where $\Omega_i = \dot{\Omega}_i = 0$,* (19) *can be obtained from the equations in [6] by choosing $P_c = 0$.*

Additionally, in Appendix V.B we provide equations for the case in which the motion of both spacecraft is restricted to the chief's orbital plane.

III. Forced equilibria under fixed angular velocity of the chief

In the following, we assume that the chief spacecraft has a constant angular velocity, i.e., that $\dot{\omega}_c = 0$.

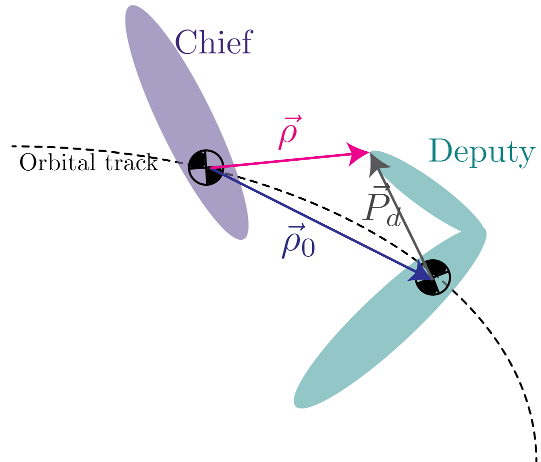

Fig. 2 Physical vectors used in the derivation of the relative dynamics.

A. Equilibria manifold for the deputy spacecraft

Given $r_t \in \mathbb{R}^3$ and $r_r \in \mathbb{R}^3$ such that $\|r_r\| \leq 1$ let $r_{q_4} \in \mathbb{R}$ be such that $\|r_{q_4}\|^2 = 1 - \|r_r\|^2$ and define

$$r = (r_t, r_r), \quad \tilde{x}(r) = (r_t, 0_{6\times 1}, r_r, r_{q_4}), \text{ and } \tilde{u}(r) = (\tilde{F}_d(r), \tilde{M}_d(r)), \text{ where} \tag{20a}$$

$$-\frac{Q^\top \tilde{F}_d(r)}{m_d} = RG_1R^\top(r_t - Q^\top P_d) + RG_2R^\top\left[\omega_c \times r_t - Q^\top(Q\omega_c \times P_d)\right] - \omega_c \times (\omega_c \times r_t) + Q^\top\left[Q\omega_c \times (Q\omega_c \times P_d)\right], \tag{20b}$$

$$-J_d^{-1}\tilde{M}_d(r) = -J_d^{-1}(\omega_c + R\omega_t) \times J_d(\omega_c + R\omega_t) + J_c^{-1}(\omega_c + R\omega_t) \times J_c(\omega_c + R\omega_t). \tag{20c}$$

Note that in (20b)-(20c) we have $Q = \mathcal{R}([r_r, r_{q_4}])$ and that, although not stated explicitly, $\tilde{F}_d(r), \tilde{M}_d(r)$ are functions of $\omega_c, [\bar{p}, p_4]$ and, therefore, of time. The latter is due to $R = \mathcal{R}([\bar{p}, p_4])$ and $[\bar{p}, p_4]$ following the dynamics in (19e)-(19f). By direct replacement, we see that $\tilde{x}(r)$, $\tilde{u}(r)$ characterize the equilibria manifold of (19) when $\dot{\omega}_c = 0$. More precisely, the equilibria manifold is parameterized by points $(\rho, \dot{\rho}, \omega, \bar{q}, q_4) = (\tilde{x}(r), r_{q_4})$, inputs $(F_d, M_d) = \tilde{u}(r)$ and letting the chief spacecraft follow its path. Note that the steady state control moments can directly be translated to RW accelerations.

B. Linearization and discretization

We now linearize (19) about a specified trimming point. A discrete-time periodic system is then obtained. For the sake of simplicity, in the controller design, instead of using the reaction wheels, we assume that control moments along each of the principal axis of the deputy spacecraft can be applied.

We linearize the EoMs (19) around the trimming point associated with the reference command, $r = 0_{6\times 1}$. The associated steady state is $\tilde{x}^0 = (0_{12\times 1}, 1)$ and the corresponding steady state control inputs are given by:

$$-\frac{F_d^0}{m_d} = -RG_1R^\top P_d - RG_2R^\top(\omega_c \times P_d) + \dot{\omega}_c \times P_d + \omega_c \times (\omega_c \times P_d), \tag{21}$$

$$-J_d^{-1}M_d^0 = -J_d^{-1}(\omega_c + R\omega_t) \times J_d(\omega_c + R\omega_t) + J_c^{-1}(\omega_c + R\omega_t) \times J_c(\omega_c + R\omega_t). \tag{22}$$

The linearization results in a linear time-varying system with states $x = (\rho, \dot{\rho}, \omega, \bar{q})$ and control inputs $u = (F_d, M_d) - \tilde{u}_0$. More precisely, the dynamics are

$$\dot{x} = A^c(t)x + B^c(t)u, \tag{23}$$

where the matrices $A^c(t)$, $B^c(t)$ are constructed using the partial derivatives given in Appendix V.A. Let T_s be an adequately chosen sampling period, see next paragraph for more information. A piecewise constant approximation of (23) is obtained by using a zero-order Taylor approximation of matrices $A^c(t)$, $B^c(t)$ at time instant kT_s. The resulting system is

$$\dot{x} = A_k^c x + B_k^c u, \quad \text{for } t \in [kT_s,\ (k+1)T_s],$$
$$\text{where } A_k^c = A^c(kT_s),\ B_k^c = B^c(kT_s).$$

A Zero-Order-Hold with sampling period T_s can then be applied to obtain a discrete time-varying linear system with dynamics

$$x_{k+1} = A_k x_k + B_k u_k. \tag{24}$$

The time-varying aspect of matrices A^c, B^c comes from the rotation of the chief spacecraft with respect to the LVLH frame, $\mathcal{T}$, which enters the dynamics through the R matrix. The system (24), in some instances, simplifies to a time-invariant system or a periodic discrete-time system. More precisely we have that:

- If $\omega_c = 0$ and $\dot{\omega}_c = 0$, then, for all choices of T_s, (24) is time-invariant.
- If the chief has a constant non-zero angular velocity, i.e., $\dot{\omega}_c = 0$ and $T_s = \frac{2\pi}{\|\omega_c\| N_T}$, where $N_T \in \mathbb{Z}_{>0}$, then (24) is periodic with period N_T.

IV. Case study - docking point estimation and control

One of the main advantages of considering the relative dynamics in the chief body fixed frame, i.e., of (19), is that tracking a relative position and relative orientation translates to tracking a constant reference command. This is the case even in the case of a rotating chief spacecraft. To illustrate the advantage, we will consider a rendezvous maneuver in which the location of the docking port on the chief spacecraft is initially unknown. In this work we do not focus on the docking port estimation problem and instead consider that, based on appropriate measurements, an oracle communicates estimates of the docking port location, alongside with an estimation error bounding set. One example of such oracle would be a DT [4] of the chief spacecraft in combination with a perception system. For this maneuver, we assume that the angular velocity of the chief, ω_c, the dimensions of the chief spacecraft and the states, $\rho, \dot{\rho}, \omega, \bar{q}, q_4$ are known. These can, for example, be estimated using the DT formalism in a previous phase of the mission.

A. System description and stabilizing controller

Both spacecraft are assumed to be cuboids. The chief has dimensions 1 by 1.2 by 1.6 meters and the deputy 0.6 by 0.6 by 0.8 meters. The chief weights 360 kg and the deputy 130 kg. Actuator saturation at 0.3 N and 0.1 Nm are considered for the control forces and moments, respectively. The docking ports are located at $P_d = (0.3, 0, 0)$ and $P_c = (-0.5, 0.2, 0.4)$. Figure 3 shows the two spacecraft with the docking ports facing each other. The discretization is performed using a sampling time, $T_s = 2$ sec. A discrete-time periodic LQR controller is designed for the resulting discrete-time periodic linear system. All simulations are performed using the periodic discrete-time linear model.

B. Maneuver description and simulation results

We start by describing the goal of the maneuver in a general setting.

Objective of the maneuver: The deputy spacecraft starts with an arbitrary position and orientation $(\rho,\ \bar{q})$ and without information regarding the position of the docking port. At the end of the maneuver, the position of the chief docking port is known, and the deputy spacecraft is in the vicinity of the chief spacecraft, the docking ports are aligned. The spacecraft are at a safe distance one from the other.

In order to achieve the objectives above, the maneuver is decomposed into four phases. While describing the different phases we will illustrate them through a rendezvous maneuver to a chief spacecraft characterized by $\omega_c = 0$.

Phase 1.a : The deputy spacecraft is brought into the vicinity of the chief. In this phase we set $r_t = r^1$ and $r_r = \bar{q}(0)$. The reference r_1 is chosen appropriately, to avoid collision and so that the perception system can capture the chief spacecraft.

Phase 1.b : Keeping the distance $\|r_1\|$, the deputy spacecraft is re-oriented relative to the chief. In this phase we set $r_t = r^1$ and $r_r = \bar{q}^1$. The target orientation $\bar{q}^1$ can be chosen freely and might be dictated by the location of the perception system. See Figure 4a.

Phase 2 : A circumnavigation of the chief is performed to determine on what side of the chief is the docking port located. To this end, a sequence of desired translational reference commands describing a circle of radius $\|r_1\|$ in frame C is computed and the deputy is set to follow this time-varying reference trajectory. The discrete sequence of references is given by $\{r_j^{(2)}\}_{j=0}^{N^{(2)}}$. We assume that the orientation of the deputy spacecraft is kept constant. See Figure 4b.

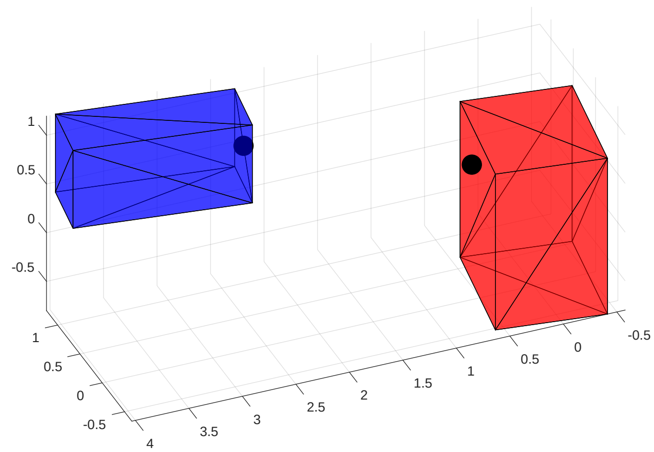

Fig. 3 Representation of the chief (red cuboid) and deputy (blue cuboid) spacecrafts as well as their docking ports (black round markers).

Phase 3 : Once the plane on which the target docking port lies has been determined, a safe trajectory is generated and the deputy moves along it. The deputy is then reoriented so as to have its docking port facing the target plane. The translational reference command trajectory is given as $\{r_j^{(3)}\}_{j=0}^{N^{(3)}}$ and the desired attitude reference command is characterized by $\bar{q}^3$. See Figure 4c.

Phase 4 : Based on the oracle estimate of the docking port position and the amount of uncertainty, the spacecraft is conservatively moved along a sequence of target translational reference commands that maintains the docking ports aligned but avoids the risk of collision. See Figure 4d.

Remark 2 *In the case where the oracle is a digital twin the trajectory generation can be integrated with the digital twin framework. A supervisory scheme, such as a periodic reference governor [8] can also be integrated to ensure constraints satisfaction and enforce collision avoidance.*

Finally, we consider a similar maneuver but assuming that the chief spacecraft is rotating at a fixed rate: $\omega_c = (0, 0, 0.01)$. Figure 5 shows an overview of the maneuver in the LVLH frame. One can observe the rotation of the chief and the more complex trajectory. Time histories of the different states (resolved in the chief body fixed frame) and inputs are shown in Figure 6

V. Conclusion and future work

In this paper we derived equations of motion (EoMs) describing the relative position of a point of interest (e.g., a docking port) on a deputy spacecraft with respect to the center of mass of a chief spacecraft assuming different actuators on the deputy spacecraft. Relative orientation dynamics were also computed. Based on the EoMs derived we considered a rendezvous maneuver assuming the position of the chief docking port was unknown. The proposed target trajectory considered different phases such as approach, determination of the docking port position and finally convergence to the chief docking port. This illustrated the advantage of the EoMs as the reference command, which is time-varying in the LVLH frame, appeared as constant in time using these dynamics. Future work will focus on constrained controllers for the nonlinear dynamics as well as on the integration of the control scheme into the digital twin framework for better controller performance.

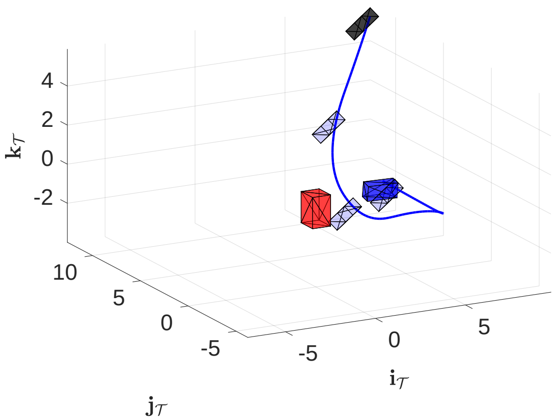

(a) Phase 1 - approach and initial re-orientation of the deputy spacecraft.

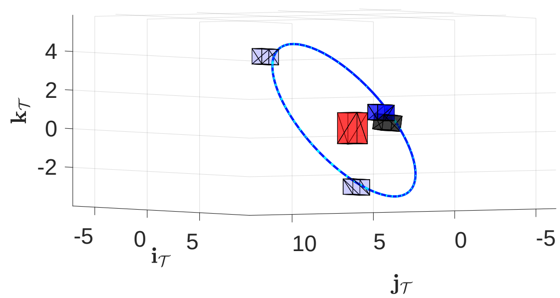

(b) Phase 2 - search for the chief docking port.

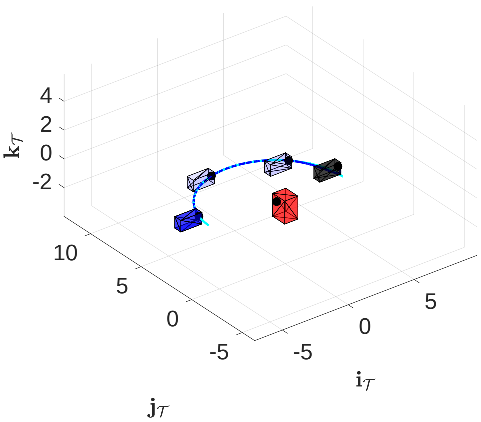

(c) Phase 3 - approaching the docking port side and reorientation.

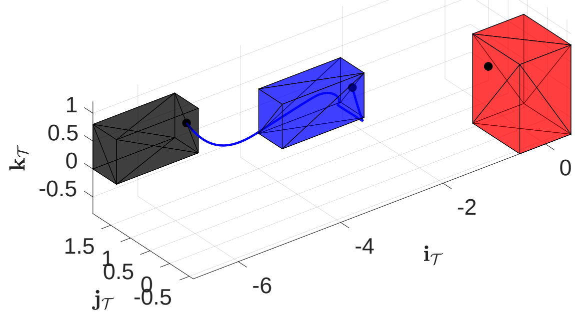

(d) Phase 4 - Precise estimation of the docking port position and further approach.

Fig. 4 Different phases of the maneuver shown in the LVLH frame $\mathcal{T}$. In all figures the chief spacecraft is the red cuboid, the deputy starting position is the black cuboid, the ending position is in dark blue and intermediary positions are shown in light blue. The trajectory of the deputy docking port is shown as a dashed blue line and a dashed cyan line represents the reference trajectory.

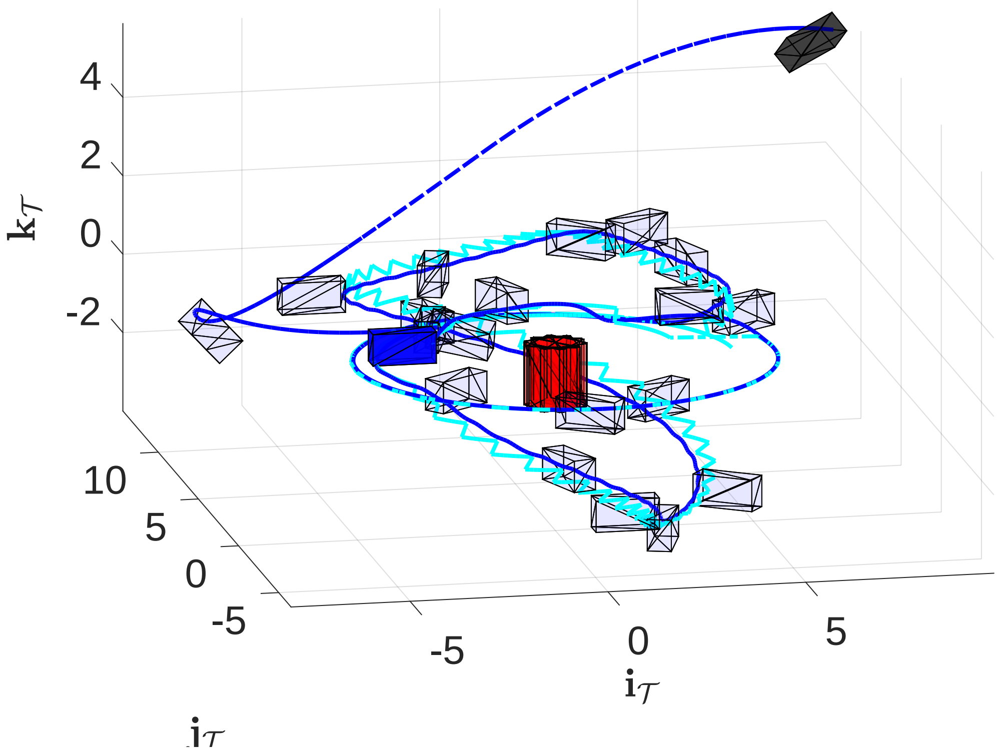

Fig. 5 Overview of the pre-capture maneuver shown in the LVLH frame, $\mathcal{T}$,considering a rotating chief spacecraft. The chief spacecraft is the red cuboid. Intermediary positions of the chief are depicted in light red. The deputy starting position is the black cuboid, the ending position is in dark blue and intermediary positions are shown in light blue. The trajectory of the deputy docking port is shown as a dashed blue line and a dashed cyan line represents the reference trajectory.

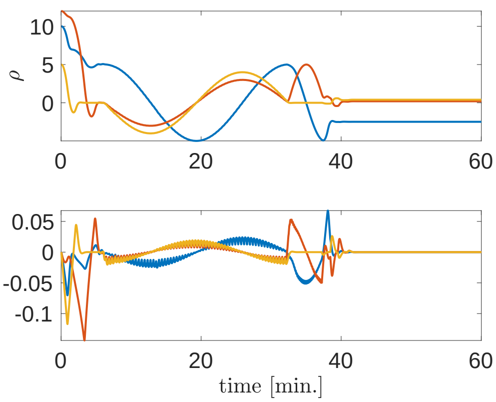

(a) Position.

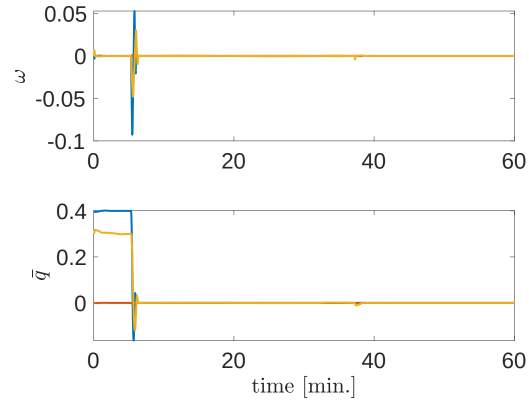

(b) Orientation.

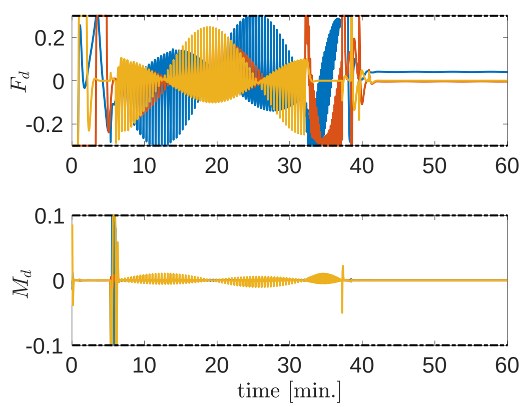

(c) Inputs.

Fig. 6 Time histories of the inputs, relative position and relative orientation resolved in the chief body fixed frame, C considering a rotating chief spacecraft.

Appendix

A. First order derivatives

In order to form the matrices $A^c(t), B^c(t)$ that describe the linearized dynamics we compute the partial derivatives of (19) with respect to the different states and evaluate them at the point $[\tilde{x}^0; \tilde{u}^0]$.

To condense the derivations, we use the notation $\frac{\partial f}{\partial v}$ where f is a vector valued function and v is a vector. The operator $\frac{\partial \cdot}{\partial v}$ returns a matrix with each column being the partial derivative of the argument with respect to the corresponding component of v. Apart from the derivatives hereunder, all other partial derivatives are null at the trim point.

$$\left.\frac{\partial Q}{\partial [\bar{q}; q_4]}\right|_{(\tilde{x}^0, \tilde{u}^0)} = \left[\begin{bmatrix} -2 \\ 0 \\ 0 \end{bmatrix}^{\times}, \begin{bmatrix} 0 \\ -2 \\ 0 \end{bmatrix}^{\times}, \begin{bmatrix} 0 \\ 0 \\ -2 \end{bmatrix}^{\times}, 2I_3 \right], \tag{25a}$$

$$\left.\frac{\partial \dot{\bar{q}}}{\partial \omega}\right|_{(\tilde{x}^0, \tilde{u}^0)} = \frac{1}{2} I_3, \tag{25b}$$

For $i = 1, \dots, 4$, let $Q^{q_i} = \frac{\partial Q}{\partial q_i}$ and $\dot{\omega}^{q_i} = \frac{\partial \dot{\omega}}{\partial q_i}$, we then have:

$$\begin{aligned}
\left.\frac{\partial \dot{\omega}}{\partial q_i}\right|_{(\tilde{x}^0, \tilde{u}^0)} =& -J_d^{-1} \left[(Q^{q_i} \omega_c + Q^{q_i} R \omega_t) \times J_d(\omega_c + R\omega_t) + (\omega_c + R\omega_t) \times J_d(Q^{q_i}\omega_c + Q^{q_i} R\omega_t) \right] \\
& + Q^{q_i} J_c^{-1} \left[(\omega_c + R\omega_t) \times J_c(\omega_c + R\omega_t) \right], \; i = 1, \dots, 4,
\end{aligned} \tag{25c}$$

$$\left.\frac{\partial \dot{\omega}}{\partial \omega}\right|_{(\tilde{x}^0, \tilde{u}^0)} = J_d^{-1} \left[(J_d \omega_c + J_d R \omega_t)^{\times} - (\omega_c + R\omega_t)^{\times} J_d \right] - (\omega_c + R\omega_t),^{\times} \tag{25d}$$

$$\left.\frac{\partial \dot{\omega}}{\partial Md}\right|_{(\tilde{x}^0, \tilde{u}^0)} = J_d^{-1}, \tag{25e}$$

$$\left.\frac{\partial \dot{\rho}}{\partial \dot{\rho}}\right|_{(\tilde{x}^0, \tilde{u}^0)} = I_3, \tag{25f}$$

$$\left.\frac{\partial \ddot{\rho}}{\partial \dot{\rho}}\right|_{(\tilde{x}^0, \tilde{u}^0)} = RG_2R^{\top} - 2\omega_c^{\times}, \tag{25g}$$

$$\left.\frac{\partial \ddot{\rho}}{\partial \rho}\right|_{(\tilde{x}^0, \tilde{u}^0)} = RG_1R^{\top} + RG_2R^{\top}\omega_c^{\times} - \dot{\omega}_c^{\times} - \omega_c^{\times}\omega_c^{\times}, \tag{25h}$$

$$\left.\frac{\partial \ddot{\rho}}{\partial \omega}\right|_{(\tilde{x}^0, \tilde{u}^0)} = RG_2R^{\top}P_d^{\times} - P_d^{\times}\frac{\partial \dot{\omega}}{\partial \omega} - P_d^{\times}\omega_c^{\times} - (\omega_c^{\times}P_d)^{\times} - \omega_c^{\times}P_d^{\times}, \tag{25i}$$

$$\begin{aligned}
\left.\frac{\partial \ddot{\rho}}{\partial q_i}\right|_{(\tilde{x}^0, \tilde{u}^0)} =& \frac{1}{m_d} Q^{q_i} F_d^0 + RG_1R^{\top}Q^{q_i}P_d + RG_2R^{\top}Q^{q_i}\omega_c^{\times}P_d + RG_2R^{\top}P_d^{\times}Q^{q_i}\omega_c \\
& + Q^{q_i}\omega_c^{\times}P_d^{\times}\omega_c - (\omega_c^{\times}P_d)^{\times}Q^{q_i}\omega_c - \omega_c^{\times}P_d^{\times}Q^{q_i}\omega_c - P_d^{\times}\dot{\omega}^{q_i}, \; i = 1, \dots, 4,
\end{aligned} \tag{25j}$$

$$\left.\frac{\partial \ddot{\rho}}{\partial F_d}\right|_{(\tilde{x}^0, \tilde{u}^0)} = \frac{I_3}{m_d}, \tag{25k}$$

$$\left.\frac{\partial \ddot{\rho}}{\partial P_c}\right|_{(\tilde{x}^0, \tilde{u}^0)} = RG_1R^{\top} + RG_2R^{\top}\omega_c^{\times} - \dot{\omega}_c^{\times} - \omega_c^{\times}\omega_c^{\times} \tag{25l}$$

B. Equations of Motion - restricted to orbital plane

We now describe a similar set of equations assuming that the motion of both the chief and deputy spacecraft is restricted to the chief spacecraft orbital plane. This entails several simplifications:

- Frames $\mathcal{I}, \mathcal{T}, \mathcal{D}, \mathcal{C}$ all have an axis pointing in the same direction referred to as $\vec{\mathbf{k}}$. We assume that one of the principal moments of inertia of each spacecraft is aligned with $\vec{\mathbf{k}}$.
- A single RW is considered.

- Let v be a mathematical vector in $\mathbb{R}^3$. Then, superscripts x, y, z denote the first, second and third component respectively. When restricting the motion to the orbital plane we then have: $\rho_0^z = \rho^z = 0$, $\omega^x = \omega_t^x = \omega_c^x = 0$, $\omega^y = \omega_t^y = \omega_c^y = 0$, $P_d^z = F_d^z = 0$ and $M_d^x = M_d^y = 0$.
- The moment of inertia of the different objects along the direction $\vec{\mathbf{k}}$ is referred to using the subscript zz.
- Instead of relying on quaternions, rotation matrices Q, R are parameterized by angles θ, β. More precisely, we have that $\omega_c^z = \dot{\theta}, \omega^z = \dot{\beta}$ and

$$Q = \begin{bmatrix} \cos\beta & -\sin\beta & 0 \\ \sin\beta & \cos\beta & 0 \\ 0 & 0 & 1 \end{bmatrix}, \quad R = \begin{bmatrix} \cos\theta & -\sin\theta & 0 \\ \sin\theta & \cos\theta & 0 \\ 0 & 0 & 1 \end{bmatrix}.$$

Define $\mathcal{A} = \begin{bmatrix} 0 & -1 & 0 \\ 1 & 0 & 0 \\ 0 & 0 & 0 \end{bmatrix}$, we then have the following relations:

- $R\mathcal{A} = \mathcal{A}R$ and $Q\mathcal{A} = \mathcal{A}Q$.
- Given that $G_1 = 2n\mathcal{A}$ we get: $RG_1R^\top = 2nR\mathcal{A}R^\top = 2n\mathcal{A}RR^\top = G_1$.
- $\mathcal{A}^2 = \begin{bmatrix} -1 & 0 & 0 \\ 0 & -1 & 0 \\ 0 & 0 & 0 \end{bmatrix}$.

C. Rotational EOMs

Starting from (19h), the rotational dynamics can be replaced by:

$$\begin{aligned}
\dot{\omega} = J_{d,zz}^{-1} &\left(M_d - (\omega + \omega_c + \omega_t) \times J_{d,zz}(\omega + \omega_c + \omega_t)\right) \\
&+ J_{c,zz}^{-1}(\omega_c + \omega_t) \times J_{c,zz}(\omega_c + \omega_t) - (\omega_c + \omega_t) \times \omega \\
&-J_{d,zz}^{-1}\left(J_{zz}^{rw}\dot{\Omega} + (\omega + \omega_c + \omega_t) \times J_{zz}^{rw}\Omega\right). \\
\implies &\begin{cases} \dot{\omega}^z & = J_{d,zz}^{-1}\left(M_d^z - J_{zz}^{rw}\dot{\Omega}^z\right), \\ \dot{\omega}^x & = 0, \\ \dot{\omega}^y & = 0 \end{cases}
\end{aligned}$$

D. Translational EoMs

Starting from (19a), the translational motion dynamics are given by

$$\begin{aligned}
\ddot{\rho} = &\ 2n\mathcal{A}\rho + RG_2R^\top\dot{\rho} + \frac{Q^\top}{m_d}F_d \\
&+ 2n\mathcal{A}Q^\top P_d + RG_2R^\top(\omega_c^z\mathcal{A}\rho - Q^\top(\omega^z + \omega_c^z)\mathcal{A}P_d) \\
&- 2\omega_c^z\mathcal{A}\dot{\rho} - \dot{\omega}_c^z\mathcal{A}\rho - \omega_c^z\mathcal{A}\omega_c^z\mathcal{A}\rho \\
&+ Q^\top\left((\dot{\omega}^z + \dot{\omega}_c^z)\mathcal{A}P_d + \omega_c^z\mathcal{A}(\omega^z + \omega_c^z)\mathcal{A}P_d\right) \\
= &\ 2n\mathcal{A}\rho + RG_2R^\top\dot{\rho} + \frac{Q^\top}{m_d}F_d \\
&- 2n\mathcal{A}Q^\top P_d + RG_2R^\top(\omega_c^z\mathcal{A}\rho - (\omega^z + \omega_c^z)\mathcal{A}Q^\top P_d) \\
&- 2\omega_c^z\mathcal{A}\dot{\rho} - \dot{\omega}_c^z\mathcal{A}\rho + (\omega_c^z)^2\rho \\
&+ (\dot{\omega}^z + \dot{\omega}_c^z)\mathcal{A}Q^\top P_d - \omega_c^z(\omega^z + \omega_c^z)Q^\top P_d \\
= &\left(2n\mathcal{A} + \omega_c^z RG_2R^\top\mathcal{A} - \dot{\omega}_c^z\mathcal{A} + (\omega_c^z)^2 I\right)(\rho - Q^\top P_d) \\
&+ (\dot{\omega}^z\mathcal{A} - \omega^z RG_2R^\top\mathcal{A} - \omega_c^z\omega^z)Q^\top P_d + \left(RG_2R^\top - 2\omega_c^z\mathcal{A}\right)\dot{\rho} + \frac{Q^\top}{m_d}F_d
\end{aligned}$$

The EOMs are summarized hereunder:

$$
\begin{aligned}
\ddot{\rho} &= \left(2n\mathcal{A} + \omega_c^z R G_2 R^\top \mathcal{A} - \dot{\omega}_c^z \mathcal{A} + (\omega_c^z)^2 I\right)(\rho - Q^\top P_d) \\
&\quad + (\dot{\omega}^z \mathcal{A} - \omega^z R G_2 R^\top \mathcal{A} - \omega_c^z \omega^z) Q^\top P_d + \left(R G_2 R^\top - 2\omega_c^z \mathcal{A}\right)\dot{\rho} + \frac{Q^\top}{m_d} F_d
\end{aligned} \tag{26a}
$$

$$
\dot{\omega} = \begin{bmatrix} 0 \\ 0 \\ J_{d,zz}^{-1}\left(M_d^z - J_{zz}^{rw}\dot{\Omega}^z\right), \end{bmatrix}. \tag{26b}
$$

$$
\dot{\beta} = \omega^z, \tag{26c}
$$

$$
\dot{\theta} = \omega_c^z \tag{26d}
$$

$$
Q = \begin{bmatrix} \cos\beta & -\sin\beta & 0 \\ \sin\beta & \cos\beta & 0 \\ 0 & 0 & 1 \end{bmatrix},\ R = \begin{bmatrix} \cos\theta & -\sin\theta & 0 \\ \sin\theta & \cos\theta & 0 \\ 0 & 0 & 1 \end{bmatrix}. \tag{26e}
$$

Acknowledgments

This research has been supported by Air Force Office of Scientific Research Grant number FA9550-23-1-0678.

References

[1] National Academy of Engineering and National Academies of Sciences, Engineering, and Medicine, *Foundational Research Gaps and Future Directions for Digital Twins*, The National Academies Press, 2024. https://doi.org/10.17226/26894.

[2] AIAA Digital Engineering Integration Committee, "Digital Twin: Definition & Value," An AIAA and AIA institute position paper, American Institute of Aeronautics and Astronautics (AIAA) and Aerospace Industries Association (AIA), 2020.

[3] Rasheed, A., San, O., and Kvamsdal, T., "Digital twin: Values, challenges and enablers from a modeling perspective," *IEEE Access*, Vol. 8, 2020, pp. 21980–22012. https://doi.org/10.1109/ACCESS.2020.2970143.

[4] Kapteyn, M. G., Pretorius, J. V., and Willcox, K. E., "A probabilistic graphical model foundation for enabling predictive digital twins at scale," *Nature Computational Science*, Vol. 1, No. 5, 2021, pp. 337–347.

[5] Clohessy, W., and Wiltshire, R., "Terminal guidance system for satellite rendezvous," *Journal of the Aerospace Sciences*, Vol. 27, No. 9, 1960, pp. 653–658.

[6] Petersen, C., and Kolmanovsky, I., "Coupled translational and rotational dynamics for precise constrained rendezvous and docking with periodic reference governors," *Proceedings of 26th AAS/AIAA Space Flight Mechanics Meeting*, Vol. 158, 2016.

[7] Segal, S., and Gurfil, P., "Effect of kinematic rotation-translation coupling on relative spacecraft translational dynamics," *Journal of Guidance, Control, and Dynamics*, Vol. 32, No. 3, 2009, pp. 1045–1050.

[8] Ossareh, H. R., "Reference governors and maximal output admissible sets for linear periodic systems," *International Journal of Control*, Vol. 93, No. 1, 2020, pp. 113–125.